ARTICLE

# Effect of Surface Protonation on Device Performance and Dye Stability of Dye-sensitized $TiO_2$ Solar Cell

Kun-jie Wu[a], Kai Shen[a], Yang Yu[a], De-liang Wang[a,b,c*]

*a. Hefei National Laboratory for Physical Sciences at the Microscale, University of Science and Technology of China, Hefei 230026, China*
*b. CAS Key Laboratory of Energy Conversion Materials, University of Science and Technology of China, Hefei 230026, China*
*c. State Key Lab of Silicon Materials, Zhejiang University, Hangzhou 310027, China*

(Dated: Received on September 26, 2012; Accepted on October 18, 2012)

A flat thin $TiO_2$ film was employed as the photo-electrode of a dye sensitized solar cell (DSSC), on which only a geometrical mono-layer of dye was attached. The effect of surface protonation by HCl chemical treatment on the performance of DSSCs was studied. The results showed that the short-circuit current $J_{sc}$ increased significantly upon the HCl treatment, while the open-circuit voltage $V_{oc}$ decreased slightly. Compared to the untreated DSSC, the $J_{sc}$ and energy conversion efficiency was increased by 31% and 25%, respectively, for the 1 mol/L HCl treated cell. $TiO_2$ surface protonation improved electronic coupling between the chemisorbed dye and the $TiO_2$ surface, resulting in an enhanced electron injection. The decreased open-circuit voltage after $TiO_2$ surface protonation was mainly due to the $TiO_2$ conduction band edge downshift and was partially caused by increased electron recombination with the electrolyte. *In situ* Raman degradation study showed that the dye stability was improved after the $TiO_2$ surface protonation. The increased dye stability was contributed by the increased electron injection and electron back reaction with the electrolyte under the open-circuit condition.

**Key words:** Dye-sensitized solar cell, Surface protonation, Electron injection, Recombination, Dye stability

## I. INTRODUCTION

Dye-sensitized solar cell (DSSC) is one of the most studied new-generation photovoltaic devices over the last two decades [1]. In a typical DSSC, the active photoelectrode is a mesoporous anatase $TiO_2$ thin film with nanocrystalline size of ∼20 nm. Such a DSSC structure has a large effective interface where dye adsorption and charge separation take place. Ru(II)-bipyridyl dye (N3) is commonly used in a high efficiency DSSC. Its excited state energy level locates well above the $TiO_2$ conduction band, leading to an efficient electron injection from excited dye to the $TiO_2$ conduction band. The electron injection rate is in a timescale of femtosecond [2]. The large network interface area, together with high electron injection rate, is believed to account for the high energy conversion efficiency. For a DSSC device, the performance is essentially determined by the material properties and interface coupling of the cell components, *i.e.*, the mesoporous $TiO_2$ network, the dye and the redox electrolyte used in a DSSC. The electronic coupling and transport process are strongly influenced and occur at the interface of $TiO_2$ and dye/electrolyte, such as electron injection from excited dyes to the $TiO_2$ conduction band, reduction of oxidized dyes and recombination between $TiO_2$ and electrolyte/dye. Figure 1 illustrates the main electron transfer/recombination processes occurred at the $TiO_2$/dye and the $TiO_2$/electrolyte interfaces. The approximate time constants/rates are also given in Fig.1 [3, 4]. It should be noted that the values of the electron kinetics rates of the different processes shown in Fig.1 varied much in the publications due to the experimental difficulties and the complexity of the processes in a DSSC [3−5]. So the DSSC device performance is therefore sensitive to the interface/surface states at the atomic/molecular level [6, 7]. Much effort has been made to modify the $TiO_2$ surface in order to improve the conversion efficiency [8−14]. It has been reported that $TiO_2$ photoelectrode treated by acid would adsorb protons on the surface. Such treatment altered the relative alignment of the energy level of dye molecule and the $TiO_2$ conduction band, and consequently promoted electron injection efficiency and increased the short-circuit current [8, 9]. Adding an energy barrier at the $TiO_2$ surface has been reported

*Author to whom correspondence should be addressed. E-mail: eedewang@ustc.edu.cn, Tel.: +86-551-3600450, FAX: +86-551-63606266

 

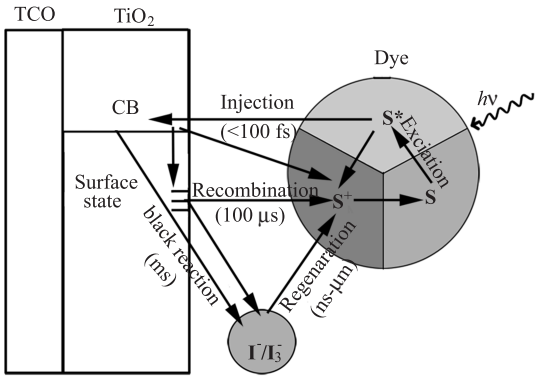


FIG. 1 Schematic diagram of electron/charge transfer processes at the $TiO_2$/dye and $TiO_2$/electrolyte interface in a DSSC and corresponding time constants.

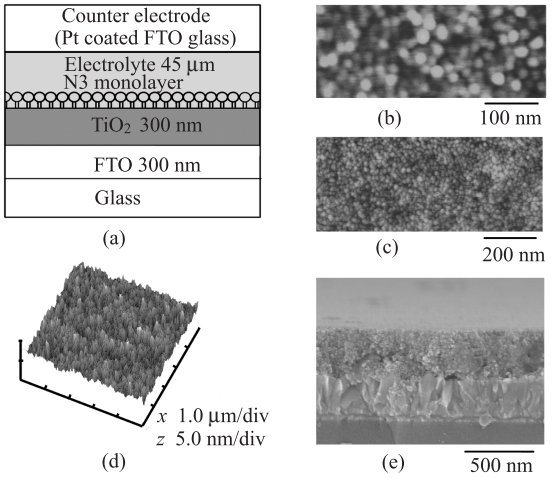


FIG. 2 (a) The DSSC structure designed in this work, (b) top-view of AFM of the FTO thin film, and (c) a 300-nm-thick $TiO_2$ thin film. (d) 3D-view of AFM of $TiO_2$ film surface, (e) cross sectional SEM image of the $TiO_2$ film.

to reduce recombination reaction and improve the solar cell performance [10, 11]. Other surface treatment technologies can also change the $TiO_2$ surface property, especially the surface states of $TiO_2$, and have been employed to modify the $TiO_2$ DSSC device. These technologies include plasma treatment [12], vacuum annealing [13], and electron-beam treatment [14]. In this study, we designed and fabricated DSSCs using thin flat $TiO_2$ films as the photoelectrodes. The purpose was to make the DSSC device structure as simple as possible, so that the factors which complicated the analysis of the processes occurred in a DSSC could be eliminated and/or mitigated. We focused on the effect of the $TiO_2$ surface protonation on the device parameters of a DSSC and the dye stability.

The commonly employed mesoporous $TiO_2$ film in a DSSC contains many grain boundaries, surface states, and lattice defects. The pore size is also not uniform, which induces different micro-environments for light scattering and ion diffusion. This leads to problems regarding to cell fabrication reproducibility, and sometimes, to inconsistent experimental results and conclusions [15, 16]. The simplified DSSC structure designed for this work is shown in Fig.2(a). The photoelectrode is made of a densely packed $TiO_2$ nanocrystalline film with a thickness of 300 nm (see Fig.2(e)) and a surface roughness of 0.76 nm (see Fig.2 (c) and (d)). The ultra-flat $TiO_2$ surface allowed only a monolayer dye to be adsorbed on the surface. Compared to the conventional DSSC structure, the DSSC structure designed in this work has the following advantages: the number of $TiO_2$ grain boundaries encountered by the injected electrons decreased dramatically; the recombination process occurred only at the $TiO_2$ film surface, while the recombination occurring within the network of a mesoporous $TiO_2$ film, was totally eliminated; the effect of the micro-environments, which induced multi-reflections of the incident light and different diffusion rates for $I^-$ and $I_3{}^-$ in a mesoporous $TiO_2$ thin film, was also absent in our devices. The most advantageous design of our DSSCs was that the surface plasmon, which was induced at the surface of the fluorine doped tin oxide (FTO) by the incident light, created a localized electric field with a tremendously high intensity [17]. The strong localized electric field was associated with the surface plasmon at the nano-structured FTO surface as shown in Fig.2(b). The electric field decreased exponentially in distance away from the FTO/$TiO_2$ interface, but relatively strong electric field could still be maintained at the surface of a thin $TiO_2$ film due to its small thickness. This strong electric field can enhance light absorption by the chemically adsorbed dyes and increase the cell efficiency [7, 18]. Such a DSSC design allowed us to fabricate solar cells with very good reproducibility [7].

## II. EXPERIMENTS

Anatase nanocrystalline thin films were prepared by sol-gel and spin-coating method [19]. Tetrabutyl titanate ($Ti(OC_4H_9)_4$), acetic acid, deionized water (DI water, 18.2 MΩ·cm), and absolute ethanol were used as the reaction precursors. The formed $TiO_2$ sol was spin-coated onto a FTO glass substrate, then a 500 °C air-annealing process was applied to crystallize the film. The as-prepared $TiO_2$ electrodes were treated with hydrochloric acid with different concentration. These $TiO_2$ electrodes were characterized by various techniques, such as scanning electron microscopy (SEM), atomic force microscopy (AFM), and X-ray photoelectron spectroscopy (XPS), *etc.* The $TiO_2$ electrodes also serve as photoelectrodes in DSSC devices. *Cis*-bis(isothiocyanato)-bis-(2,2′-bipyridyl-4,4′-dicarboxylic acid)-ruthenium(II) (N3) dye was used as the light absorber. The $TiO_2$ electrodes were im-

DOI:10.1088/1674-0068/25/06/733-738 

mersed in a dye ethanol solution (0.2 mg/mL) for 12 h at room temperature to adsorb dye molecules. A drop of redox electrolyte, which consisted of 0.1 mol/L LiI, 0.12 mol/L $I_2$, 1 mol/L 1,2-dimethylpropylimidazolium iodide (DMPII), and 0.5 mol/L 4-*tert*-butylpyridine (4-TBP) in 3-methoxypropionitrile, was introduced into the cell via vacuum backfilling from a hole made on the counter electrode. The active cell area was 0.16 $cm^2$. The detailed DSSC device fabrication process can be found in our previous work [7]. The DSSCs with different acid-treated photoelectrodes were characterized by means of light *I-V* and dark-*I-V* measurements and the electrochemical impedance spectroscopy. *In situ* Raman spectroscopy measurement for dye degradation was carried out under open-circuit condition. The 514 nm exciting laser had a power of 2.2 mW, corresponding to a light intensity of $\sim 10^8$ W/$m^2$, about five orders higher than that of the one-sun irradiation ($\sim 10^3$ W/$m^2$ at AM 1.5). The high intensity laser light would accelerate dye degradation. This allowed us to study the effect of surface protonation on dye stability in a very short test time.

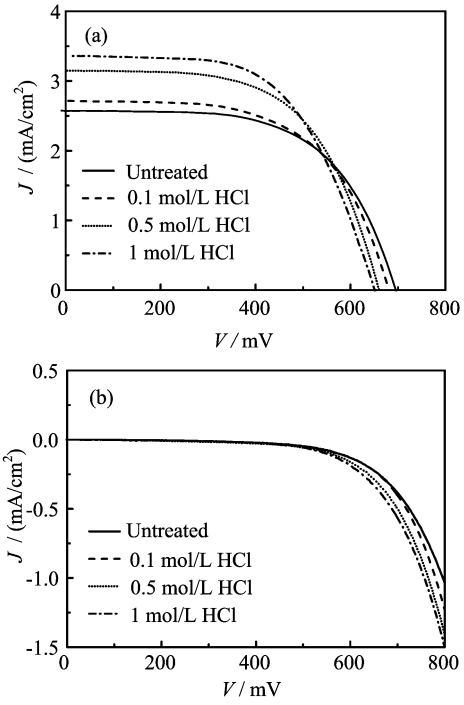


FIG. 3 (a) *J-V* curves under AM 1.5 illumination of DSSCs based on $TiO_2$ treated by hydrochloric acid with different concentration. (b) *J-V* curves in the dark of the corresponding samples.

## III. RESULTS AND DISCUSSION

The surface protonation was done by immersing $TiO_2$ films into hydrochloric acid aqueous solution with concentrations of 0.1, 0.5, and 1 mol/L for 1 h. The electrodes were then rinsed with DI water and dried in air at 60 °C for 1 h. The $TiO_2$ surface morphologies and microstructure were characterized by atomic force microscopy and X-ray diffraction. The $TiO_2$ films had a homogeneous grain size distribution centered at 20 nm and a root-mean-square surface roughness of 0.76 nm (see Fig.2 (c) and (d)). The photocurrent-voltage characteristics of the devices were measured under a standard AM 1.5 condition, which are shown in Fig.3(a). The cell efficiency with an untreated $TiO_2$ film is 1.08%. Such an energy conversion efficiency is relatively high for a DSSC with only a geometrical mono-layer dye attached to a flat $TiO_2$ film. The conversion efficiency remained below 1% for a DSSC using a flat-surface photoelectrode before a mesoporous $TiO_2$ film began to be used as the photoelectrode for a DSSC [1]. In a mesoporous DSSC the nanocrystalline $TiO_2$ film, with a thickness of $\sim$ 10 μm, adsorbs a large amount of dye molecules, about 600 times higher than that adsorbed on an ultra-flat $TiO_2$ surface. This huge amount of dyes ensures a short-circuit current as large as $\sim$22 mA/$cm^2$ [20]. It can be seen from Fig.3(a) that the 1 mol/L HCl treated solar cell has a short-circuit current of 3.37 mA/$cm^2$. Considering that only a geometrical monolayer of N3 dye was adsorbed on the flat $TiO_2$ film, such a value of short-circuit current is an evidence of an enhanced localized electric field, which enhanced the light absorption. Increased short-circuit current after HCl surface treatment was also reported by other researchers [21, 22]. The $J_{sc}$ were 2.58, 2.71, 3.15, and 3.37 mA/$cm^2$ for the untreated, 0.1, 0.5, and 1 mol/L HCl treated solar cells, respectively. Compared to the untreated solar cell, the $J_{sc}$ of the 1 mol/L HCl treated one was increased by 31%. This current increase was induced by enhanced electron injection from the excited dye to the $TiO_2$ conduction band [21−23]. The attachment of the positively charged $H^+$ on the $TiO_2$ surface moved its conduction band downwards, and therefore the chemical potential driving force for the electron injection was increased. With increased HCl concentration for the surface treatment, the amount of dye adsorbed on the $TiO_2$ surface decreased slightly, as shown in the Fig.4. Our results clearly show that the increased $J_{sc}$ was caused by the increased electron injection, not due to an increased amount of the adsorbed dye, as reported by Qu *et al.* [24]. The amount of dye adsorbed on the 1 mol/L HCl treated $TiO_2$ surface was about 10% less than that on the untreated $TiO_2$ surface. Therefore compared to the untreated solar cell, the contribution of each dye molecule to $J_{sc}$ was actually increased $\sim$45% for the 1 mol/L HCl treated one.

The energy conversion efficiency $\eta$ increased significantly after surface protonation from 1.08%, to 1.14%, 1.22%, 1.35%, the fill factor remained almost unchanged, which was 0.60, 0.62, 0.59, 0.62, and the open-circuit voltage $V_{oc}$ decreased from 695 mV, to 680, 660, and 651 mV, for the untreated and 0.1, 0.5, 1 mol/L HCl treated solar cells, respectively. The increased efficiency

DOI:10.1088/1674-0068/25/06/733-738 

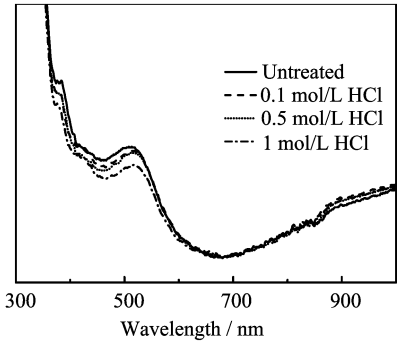


FIG. 4 UV-Vis absorption spectra of dye-sensitized $TiO_2$ electrodes treated by hydrochloric acid with different concentration.

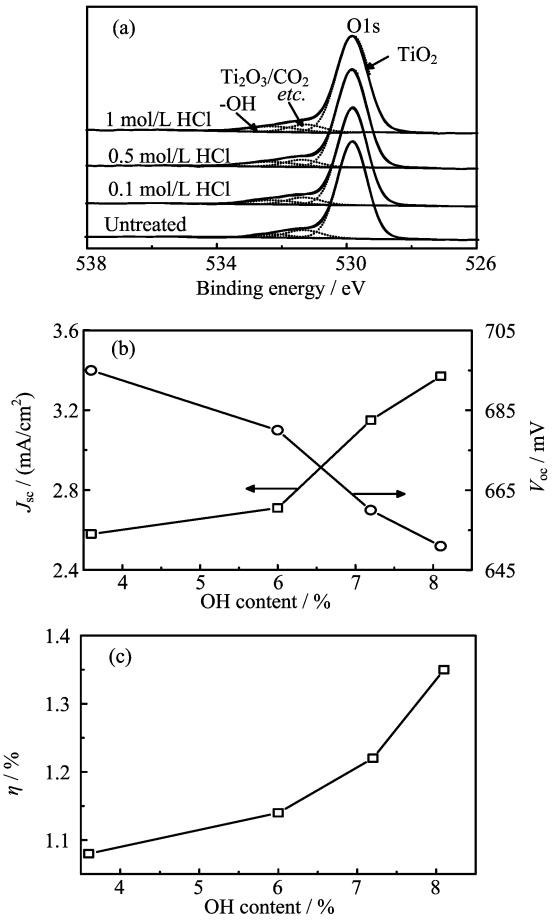


FIG. 5 (a) High resolution XPS O1s spectra of $TiO_2$ electrodes (before dye adsorption) treated by hydrochloric acid with different concentration. (b) $J_{sc}$ and $V_{oc}$ versus the OH-related O atomic concentration. (c) $\eta$ versus the OH-related O atomic concentration.

was mainly contributed by the significantly increased $J_{sc}$. After the surface HCl treatment, the leakage current was increased, as shown by the dark $J$-$V$ curves in Fig.3(b). The increased leakage current was caused by increased overlap of the $TiO_2$ conduction band states with the energy levels of the oxidized redox species in the electrolyte [25]. Surface protonation made the $TiO_2$ surface to be positively charged and lowered the conduction band edge, causing an increased energy level overlap. The decrease of $V_{oc}$ was contributed by both the downshift of the $TiO_2$ conduction band edge and the increase of leakage current. Calculated from the leakage current data of the untreated and the 1 mol/L HCl treated solar cells, the $V_{oc}$ decrease due to the increase of leakage current is only 9 mV. Therefore, 35 mV of the total 44 mV decrease in $V_{oc}$ for the 1 mol/L HCl treated solar cell is contributed by the conduction band edge downshift.

The modified $TiO_2$ surface chemical states were quantitatively analyzed by high resolution XPS. Three component peaks were employed to fit the O1s state in Fig.5(a). The main peak at ∼530.0 eV corresponds to the lattice oxygen of $TiO_2$ [26]. The relatively broad shoulder peak near 531.5 eV comes from oxygen of oxygen vacancy-$Ti^{3+}$ state ($Ti_2O_3$) and other adsorbed molecules containing oxygen [12, 27]. The peak at ∼532.5 eV comes from the OH group originating from the surface protonation [28, 29]. $J_{sc}$ and $V_{oc}$ strongly depended on the OH concentration, which was calculated from the fitting results of the XPS data, as shown in Fig.5(b). The data in this work demonstrate that the $TiO_2$ surface protonation has two effects on the DSSC device performance, namely, a much increased $J_{sc}$ and a slightly decreased $V_{oc}$. The presence of $H^+$, on one hand, enhanced the electronic coupling between the adsorbed dye and the $TiO_2$ surface. On the other hand, it enhanced intermolecular charge transfer across the nanocrystalline surface [24]. This would lead to in-plane current shunting and increased leakage current. The surface protonation also caused a slight red shift of the absorption peaks of dye, as shown in Fig.4, which was induced by the stabilized $\pi^*$ levels of bipyridine [24].

To further investigate the interfacial electron transfer dynamics of DSSCs, we carried out electrochemical impedance spectroscopy (EIS) measurements, a powerful technique to study the kinetics of electrochemical and photo-electrochemical processes occurred in a DSSC [30]. The EIS spectra of DSSCs treated with different HCl concentration are shown in Fig.6. A forward bias of 0.75 V was applied during the test, and the test frequency ranged from $10^5$ Hz to 1 Hz. There were two semicircles for each EIS spectrum. The smaller one in the high frequency region, $10^5-10^3$ Hz, was assigned to charge transfer processes occurring at the Pt/electrolyte interface. And the bigger one in the low frequency region, $10^3-1$ Hz, could be attributed to electron back transfer at the $TiO_2$/electrolyte interface, or electron transport process in $TiO_2$ nanocrystalline film [30, 31]. In this work, the acid treatments mainly changed the $TiO_2$ surface property, so the variation in the EIS spectra were caused by different electron transfer processes

DOI:10.1088/1674-0068/25/06/733-738 

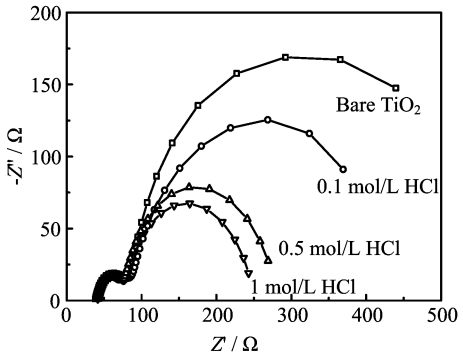


FIG. 6 EIS spectra of DSSCs based on bare $TiO_2$ and $TiO_2$ electrodes treated by hydrochloric acid with different concentration.

at the $TiO_2$/electrolyte interface. As can be seen from Fig.6, the size of the low frequency semicircle decreased with increasing the HCl concentration of acid treatment. In the Nyquist plot of a DSSC, a bigger low frequency semicircle means a weaker electron recombination at the $TiO_2$/electrolyte interface [32]. So a conclusion can be drawn that the recombination current at the $TiO_2$/electrolyte interface was increased with the increasing HCl concentration for acid treatment. This observation is consistent with the increased dark leakage current shown in Fig.3(b).

The dye stability is crucial for long-term operation of a DSSC. In this work, we employed *in situ* Raman spectroscopy to investigate degradation of dye adsorbed on untreated and HCl treated $TiO_2$ electrodes under Raman laser illumination. Resonant Raman spectroscopy is a very powerful tool for the investigation of dye-sensitized $TiO_2$ system [19, 33]. When the exciting laser wavelength matches with the metal-to-ligand charge transfer transition, resonant Raman scattering occurs, resulting in a much enhanced scattering intensity. Resonant Raman scattering condition, together with the localized strong electric field associated with the surface plasmon discussed above, makes that even a monomolecular layer adsorbed on $TiO_2$ can be easily detected by the Raman scattering. Figure 7(a) shows the Raman spectra of the dye-sensitized $TiO_2$ electrode treated with 1 mol/L HCl. The Raman spectra were taken successively with different laser illumination time. The relatively strong peak at 1544 $cm^{-1}$ of the N3 dye was used for quantitative analyses of dye degradation. The peak at 1544 $cm^{-1}$ corresponds to the carbon-carbon double bond stretching vibration. Its integral peak intensity was obtained by fitting the peak with a Lorentzian function. The curves of normalized peak intensity versus laser exposure time are shown in Fig.7(b). When the peak intensity decreases, it means that the population of bipyridine rings decreases. It can be due to the rupture or release of the bipyridine rings. It can also be due to desorption of the dye molecule from the $TiO_2$ surface. The data in Fig.7(b) can be well fitted

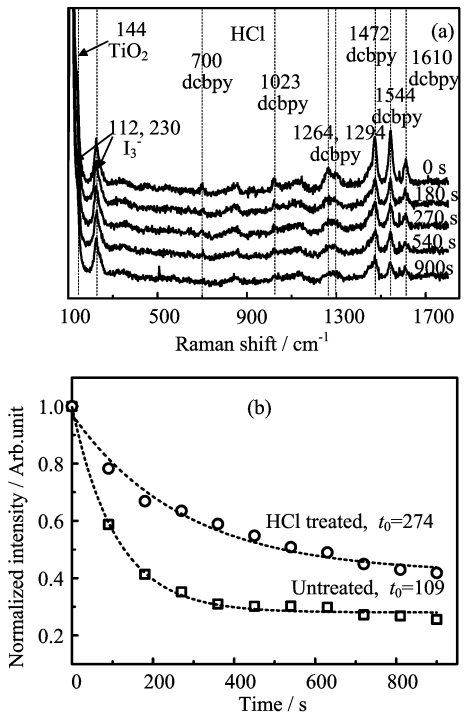


FIG. 7 (a) Raman spectra with different laser exposure time of dye-sensitized $TiO_2$ treated with 1 mol/L HCl. (b) Decay curves of the normalized 1544 $cm^{-1}$ peak intensity for the untreated and 1 mol/L HCl treated samples.

using a first-order exponential decay function:

$$I = I_0 \exp\left(\frac{-t}{t_0}\right) + A_0 \tag{1}$$

where $I_0$ and $A_0$ are constants related to the Raman signal intensity, and $t_0$ is a parameter characterizing decay rate of the dye under laser radiation, we call it decay-rate parameter.

Dyes adsorbed on the untreated and the HCl chemically treated $TiO_2$ electrodes showed similar dye degradation behavior. Therefore, only the Raman spectra for 1 mol/L HCl treated sample were shown in Fig.7(a). The dye decay-rate parameter $t_0$, derived by fitting the data using Eq.(1), differs considerably for the untreated and the protonated $TiO_2$ electrodes. Compared to the untreated electrode, the decay-rate parameter $t_0$ is 2.5 times larger for the 1 mol/L HCl treated electrode, meaning a much decreased degradation rate considering that the degradation law obeys an exponential function. N3 dye stability critically depends on $TiO_2$ chemical state and local environment in a DSSC. Ruthenium complexes may only sustain no more than 100 electron transfer processes in a solution [34], while it can sustain $10^7-10^8$ redox cycles before irreversible degradation occurs when it is properly bonded to the $TiO_2$ surface [35]. It is generally believed that the dye in excited and oxidized states is most vulnerable to degradation [36]. According to the discussion above, the electron injec-

DOI:10.1088/1674-0068/25/06/733-738 

tion rate for the dye adsorbed on the HCl treated $TiO_2$ electrode was enhanced compared to that bonded on the untreated one [23]. The dye molecule would then stay in the excited state for a shorter time and consequently had less chance to suffer irreversible degradation. For the decay route via the oxidized state, the irreversible degradation reaction competed with the regeneration process of the dye by the $I^-$ anion in the electrolyte. Under open circuit condition, the injected electrons could not transport to the counter electrode through the external circuit to reduce the $I_3{}^-$ iodide, rather they had enhanced chance to back react with the $I_3{}^-$ to produce $I^-$, which then regenerated the oxidized dye. As can be seen in Fig.3(b), the HCl treated cells had an increased electron back reaction rate compared with the untreated one, leading to an increased $I^-$ generation and thus decreased dye degradation via the oxidized state. These two effects reduced the degradation rate of the dye adsorbed on the HCl treated $TiO_2$ electrode.

## IV. CONCLUSION

$TiO_2$ surface protonation by HCl acid treatment resulted in improved electronic coupling between the chemisorbed dye sensitizer and the $TiO_2$ surface, which enhanced the photo-generated electron injection from the dye to the $TiO_2$ electrode and resulted in a much increased short-circuit current. Compared to the untreated DSSC, the short-circuit current and the energy conversion efficiency was increased by 31% and 25%, respectively, for the 1 mol/L HCl treated cell. The decreased open-circuit voltage after $TiO_2$ surface protonation was mainly due to the $TiO_2$ conduction band edge downshift and was partially caused by increased electron recombination with the electrolyte. The surface protonation by HCl treatment also improved the dye stability under open-circuit condition.

## V. ACKNOWLEDGMENT

This work was supported by the National Natural Science Foundation of China (No.60976054 and No.51272247).

[1] B. O'Regan and M. Grätzel, Nature **353**, 737 (1991).
[2] J. Kallioinen, G. Benkö, P. Myllyperkiö, L. Khriachtchev, B. Skårman, R. Wallenberg, M. Tuomikoski, J. Korppi-Tommola, V. Sundström, and A. P. Yartsev, J. Phys. Chem. B **108**, 6365 (2004).
[3] A. Hagfeldt and M. Grätzel, Chem. Rev. **95**, 49 (1995).
[4] H. J. Snaith and L. Schmidt-Mende, Adv. Mater. **19**, 3187 (2007).
[5] A. N. M. Green, E. Palomares, S. A. Haque, J. M. Kroon, and J. R. Durrant, J. Phys. Chem. B **109**, 12525 (2005).
[6] J. Weidmann, T. Dittrich, E. Konstantinova, I. Lauermann, I. Uhlendorf, and F. Koch, Sol. Energy Mater. Sol. Cells **56**, 153 (1999).
[7] Y. Yu, K. Wu, and D. Wang, Appl. Phys. Lett. **99**, 192104 (2011).
[8] Z. S. Wang and G. Zhou, J. Phys. Chem. C **113**, 15417 (2009).
[9] D. F. Watson, A. Marton, A. M. Stux, and G. J. Meyer, J. Phys. Chem. B **107**, 10971 (2003).
[10] E. Palomares, J. N. Clifford, S. A. Haque, T. Lutz, and J. R. Durrant, Chem. Commun. 1464 (2002).
[11] J. Xia and S. Yanagida, Sol. Energy **85**, 3143 (2011).
[12] K. H. Park and M. Dhayal, Electrochem. Commun. **11**, 75 (2009).
[13] P. W. Chou, Y. S. Wang, C. C. Lin, Y. J. Chen, C. L. Cheng, and M. S. Wong, Surf. Coat. Technol. **204**, 834 (2009).
[14] T. Kado, M. Yamaguchi, Y. Yamada, and S. Hayase, Chem. Lett. **32**, 1056 (2003).
[15] J. M. Kroon, N. J. Bakker, H. J. P. Smit, P. Liska, K. R. Thampi, P. Wang, S. M. Zakeeruddin, M. Grätzel, A. Hinsch, S. Hore, U. Wurfel, R. Sastrawan, J. R. Durrant, E. Palomares, H. Pettersson, T. Gruszecki, J. Walter, K. Skupien, and G. E. Tulloch, Prog. Photovol: Res. Appl. **15**, 1 (2007).
[16] H. Tributsch, Coord. Chem. Rev. **248**, 1511 (2004).
[17] W. L. Barnes, A. Dereux, and T. W. Ebbesen, Nature **424**, 824 (2003).
[18] H. A. Atwater and A. Polman, Nat. Mater. **9**, 205 (2010).
[19] D. Wang, G. Wang, J. Zhao, and B. Chen, Chin. Sci. Bull. **52**, 2012 (2007).
[20] M. Grätzel, Nature **414**, 338 (2001).
[21] Z. S. Wang, F. Y. Li, and C. H. Huang, J. Phys. Chem. B **105**, 9210 (2001).
[22] Z. S. Wang, T. Yamaguchi, H. Sugihara, and H. Arakawa, Langmuir **21**, 4272 (2005).
[23] D. F. Watson and G. J. Meyer, Coord. Chem. Rev. **248**, 1391 (2004).
[24] P. Qu and G. J. Meyer, Langmuir **17**, 6720 (2001).
[25] S. Rühle, M. Greenshtein, S. G. Chen, A. Merson, H. Pizem, C. S. Sukenik, D. Cahen, and A. Zaban, J. Phys. Chem. B **109**, 18907 (2005).
[26] X. Cheng, X. Yu, and Z. Xing, Appl. Surf. Sci. **258**, 3244 (2012).
[27] J. Kunze, L. Müller, J. M. Macak, P. Greil, P. Schmuki, and F. A. Müller, Electrochim. Acta **53**, 6995 (2008).
[28] P. Supphasrirongjaroen, W. Kongsuebchart, J. Panpranot, O. Mekasuwandumrong, C. Satayaprasert, and P. Praserthdam, Ind. Eng. Chem. Res. **47**, 693 (2008).
[29] Q. Xiao, J. Zhang, C. Xiao, Z. Si, and X. Tan, Sol. Energy **82**, 706 (2008).
[30] L. Han, N. Koide, Y. Chiba, and T. Mitate, Appl. Phys. Lett. **84**, 2433 (2004).
[31] R. Kern, R. Sastrawan, J. Ferber, R. Stangl, and J. Luther, Electrochim. Acta **47**, 4213 (2002).
[32] S. Wu, H. Han, Q. Tai, J. Zhang, S. Xu, C. Zhou, Y. Yang, H. Hu, B. Chen, and X. Zhao, J. Power Sources **182**, 119 (2008).
[33] H. Greijer, J. Lindgren and A. Hagfeldt, J. Phys. Chem. B **105**, 6314 (2001).
[34] R. Grünwald and H. Tributsch, J. Phys. Chem. B **101**, 2564 (1997).
[35] O. Kohle, M. Grätzel, A. F. Meyer, and T. B. Meyer, Adv. Mater. **9**, 904 (1997).
[36] M. Grätzel, C. R. Chimie **9**, 578 (2006).

DOI:10.1088/1674-0068/25/06/733-738 